Gomez Rojas, O., Song, G., & Hall, S. (2017). Fast and scalable synthesis of strontium niobates with controlled stoichiometry. *CrystEngComm*, *36*, 5351-5355. https://doi.org/10.1039/C7CE01298E

CrystEngComm

Accepted Manuscript

This article can be cited before page numbers have been issued, to do this please use: O. Gomez, G. Song and S. Hall, *CrystEngComm*, 2017, DOI: 10.1039/C7CE01298E.

ROYAL SOCIETY OF CHEMISTRY

rsc.li/crystengcomm

View Article Online
DOI: 10.1039/C7CE01298E

Journal Name

COMMUNICATION

Fast and Scalable Synthesis of Strontium Niobates with Controlled Stoichiometry

Received 00th January 20xx,
Accepted 00th January 20xx

DOI: 10.1039/x0xx00000x

www.rsc.org/

Omar Gomez[a,b], Ge Song[a,b] Simon R. Hall*[a,b]

Recently a new method for the synthesis of metal oxides has been reported, using ionic liquids as an effective metal cation solvent and chelating agent. Here we discuss the mechanism of action of this technique and demonstrate its efficacy as a means to synthesise phase-pure strontium niobates of controlled stoichiometry.

Complex functional materials can be synthesized by a wide range of techniques. Some of these syntheses tend to be highly time and energy consuming however, raising the overall expense of the process. In addition, having control over the homogeneity of the sample can be a hard task to attain. The rapid progress of technological developments in ferroelectric[1], ferromagnetic[2], superconducting[3], and piezoelectric[4] materials demand the discovery of new synthetic routes to create materials with high efficiency. As a result of this, different synthetic approaches have been developed, among which solid-state reactions are without doubt the most commonly used, with well-established conditions and a fairly simple methodology. A feature of these reactions is that mass transport tends to be poor however and therefore formation of the desired target phase may require long synthesis times or simply may not occur.

An alternative route is the hydrothermal method. Some key features of this process are the ability to synthesize ultrafine particles; morphology can be relatively controlled to some extent through tuning pressure or temperature and control over stoichiometry is possible through reducing or oxidizing atmospheres, provided via adding extra components or gases[5]. Recently, work has been done on the combination of sol-gel and hydrothermal methods. Combining features of both techniques, the sol-gel-hydrothermal method has achieved very interesting results in synthesis of metal oxides[6,7]. This technique has become an attractive tool as advantages range from a high degree of crystallinity, good control over the morphology, high purity and a more even particle size distribution, coupled with a reduction of time and temperature needed to obtain such materials[8,9]. Disadvantages come however from the complexity of the synthesis and a poor understanding of the mechanism of action as it is hard to monitor the reaction process in an enclosed environment.

Another interesting alternative method to synthesize complex functional materials is the molten salt synthesis (MSS). Compared to solid state reactions, MSS lowers significantly the reaction temperature as it allows faster mass transport in the liquid phase. Furthermore, MSS is good at solvating metals and oxides at high temperature owing to a destabilization of bonding by the strong polarizing forces provided by the salt melts. MSS has the additional advantage of low cost and low toxicity as well as abundant availability[10].

Perhaps the most actively researched method in recent years is sol-gel chemistry. Broadly, this the preparation of inorganic phases from a transformation of liquid precursors to a sol and finally to a network structure called a gel[11]. Sol-gel chemistry has been widely used due to its ability to generate chemically homogeneous precursors allowing atomic level mixing of reagents. It is worth noting however that this does not ensure homogeneity throughout a reaction; having randomly well-distributed precursors does not necessarily guarantee an optimal reaction process. One way to improve upon a solution-based synthetic approach is to use ionic liquids. An Ionic liquid (IL) is composed of an intimate mixture of long-chain cations and coordinating anions[12]. These compounds have been described as “green” and “super-dissociating” solvents, providing an environmentally friendly way to completely solvate inorganic salts[13]. Moreover, ILs can work as templates and precursors, as they have good thermal stability, tuneable solubility, fairly low vapour pressure[14], as well as enabling fast mass transport. ILs have already proven to be a great tool in the synthesis of nanoparticles[15], metal salts[16], metal oxides and metal chalcogenides[17–20], silicas and organosilicas[21,22]. ILs have been used to synthesize multi-element complex

[a] The Bristol Centre for Functional Nanomaterials, University of Bristol, BS8 1FD
[b] Complex Functional Materials Group, School of Chemistry, University of Bristol, BS8 1TS.

† This work was supported by the Engineering and Physical Sciences Research Council (EPSRC), UK (grant EP/G036780/1).

View Article Online
DOI: 10.1039/C7CE01298E

functional oxides, creating phase pure superconductors,

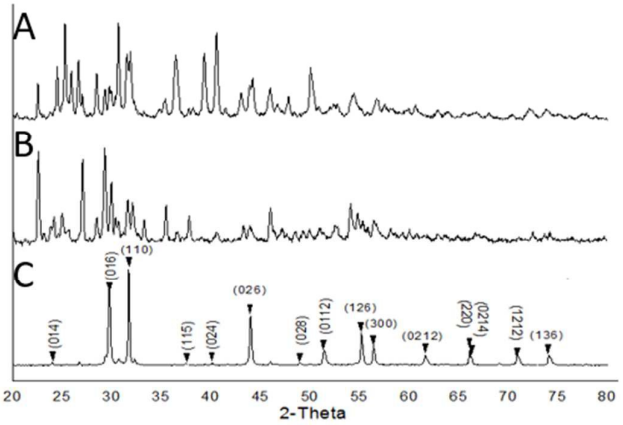

Figure 1.: Powder X-ray diffraction pattern of the synthesis of $Sr_5Nb_4O_{15}$ with (A) dextran and C) (emim)OAc as chelating agents. B) represents a control synthesis using no chelating agents.

piezoresponsive, multiferroic, ferromagnetic and phosphorescent materials[23]. Another advantage to using ILs is that it is possible to solubilise other non-specific chelating agents such as biopolymers within them, thereby increasing the chelating ability of the system.

Strontium Niobates have been widely studied for several reasons and find application in a wide range of areas. One of the most interesting yet to be exploited is the possibility of forming a new family of high temperature superconductors[3]. A Strontium niobate oxide was also the first metallic oxide-type material to be used as an effective photocatalyst[24,25]. Further properties that this materials exhibit range from large thermal expansion coefficients and low thermal conductivity[26], high frequency dielectric properties[27], piezoelectric and electro-optic properties[28,29], and photoluminescence[30]. Also, it finds use as the key component in diamagnetic insulators[31], and ferroelectricss[32,33]. Such diversity is generated from the two possible arrangements of the NbO_6 octahedra, giving rise to perovskites, ABO_3, and pyrochlore, $A_2B_2O_7$, crystal structures[34]. The physical properties are stoichiometry dependent and so control over this is highly sought after in strontium niobates.

In this work, samples of strontium niobates of controlled stoichiometries were prepared using strontium nitrate (99 %), niobium ethoxide (99.95 %), 1-Ethyl-3-methylimidazolium acetate (emim)OAc (95 %) and dextran from *Leuconostoc sp*. (molecular weight 70,000 Da). All materials were purchased from Sigma-Aldrich UK. Deionized water was obtained using a MilliQ PureLab Ultra (18.2 M Ω cm-1). None of the materials required further purification and were used as received. A typical synthesis can be described as follows: Strontium nitrate (99 %) (1 mL, 0.1 M) was added to 1 mL (emim)OAc under stirring until evenly dispersed. The whole was then heated to 80 °C in an alumina crucible under stirring to remove water from the mixture for 1 to 2 hr. Niobium ethoxide (99.95 %) was then added. The mixture remained under heating and constant stirring for one further hour, ensuring full dehydration of the system. Finally, dextran was added as a weakly coordinating, nonspecific chelating agent, (1 g) and mechanically mixed until a dense paste-like gel was formed. This was done to avoid metal specific or preferential chelation and enhance homogeneity in the system. Adding a carbon source into the reaction also serves a second purpose, as carbonization occurs over the calcination process, thereby providing a cocooning environment which prevents the sintering of crystallites restricting them to the nanoscale, thereby enhancing reactivity. Moreover, dextran provides a reducing atmosphere, generating CO_2 as the carbon is oxidised over the course of the synthesis, preventing the formation of refractory fully-oxidised impurity phases. All dehydrated precursors were calcined immediately after preparation in air in crucibles for 2 hr with a heating ramp rate of 5 °C/min at 1000 °C. The characterization of the final samples involves determination of phase type and purity by powder X-ray diffraction (pXRD), scanning and transmission electron microscopy (SEM and TEM), selected area electron diffraction (SAED) and energy dispersive X-ray analysis (EDX).

TEM analysis was carried out on JEOL JEM 1400EX microscope equipped with an Oxford energy dispersive X-Ray detector. SEM samples were analysed on JEOL JSM 5600LV with Oxford energy dispersive X-Ray. X-ray diffraction was carried out on Bruker D8 Advance diffractometer (CuKα radiation at λ = 1.54056 Å) equipped with a Lynx-eye position sensitive detector.

View Article Online
DOI: 10.1039/C7CE01298E

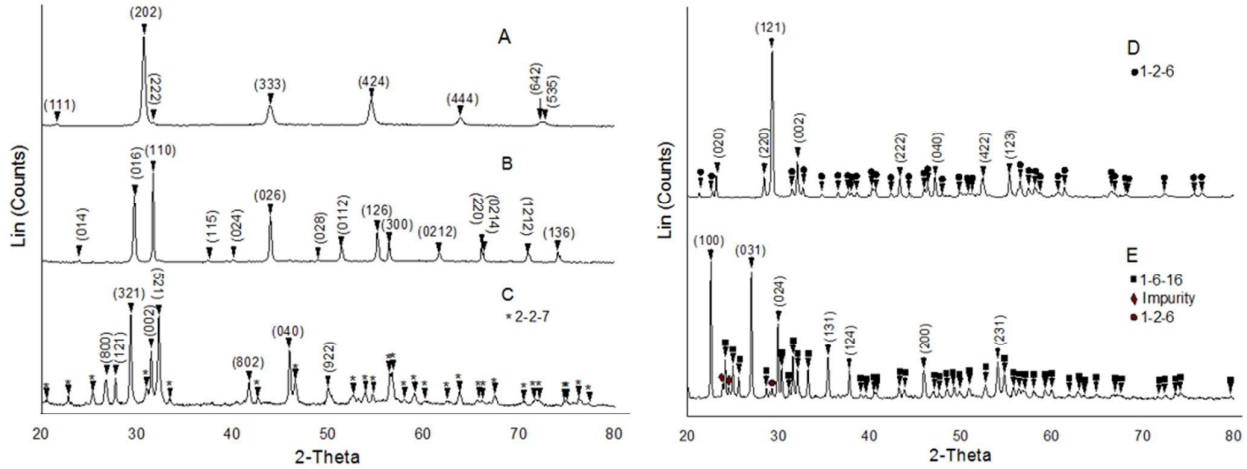

Figure 2. Powder X-ray diffraction patterns of: $Sr_4Nb_2O_9$ (A), $Sr_5Nb_4O_{15}$ (B), $Sr_2Nb_2O_7$ (C), $SrNb_2O_6$ (D) and $SrNb_6O_{16}$ (E).

To establish the crystal phase and purity of each synthesis, powder X-ray diffraction patterns were taken (Figure 1). All reactions were carried out using 1:1Sr/Nb stoichiometry targeting the phase $Sr_5Nb_4O_{15}$. For the control synthesis, strontium nitrate and niobium ethoxide were mixed in an alumina crucible and calcined. As can be seen from Figure 1, the outcome is a multiphase system with no predominant phase, as did the synthesis using dextran as the sole chelating agent. Interestingly, a different polyphasic result is seen when dextran is used. In the case where IL plus dextran was used, the target phase is obtained in a practically pure phase fashion. However, it is important to mention that this reaction was repeated several times and in some of them the outcome was a mixture of $Sr_5Nb_4O_{15}$ and $Sr_2Nb_2O_7$. In addition, for rich in niobium crystal phases, namely $SrNb_2O_6$ and $SrNb_6O_{16}$, pure phases were not able to be obtained without the use of an additional chelating agent such as dextran[35,36]. Therefore, it is clear that the best combination to obtain pure phases with controllable stoichiometry was to use the IL with addition of dextran.

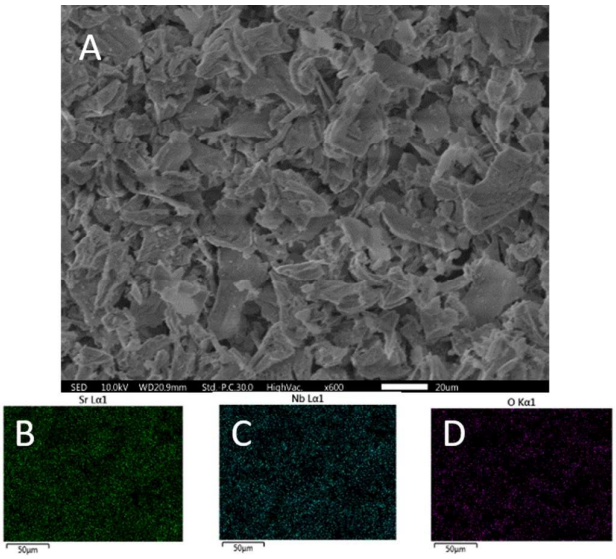

Figure 3. (A) Scanning Electron microscopy image of SrNbOx and (B-D) EDX elemental mapping of the area shown in (A).

Thermogravimetric analysis (Supplementary information, Figure S1A) of a typical synthesis (IL with dextran) shows a mass loss of just 12.18 % at 250 °C. Being a water free system, this mass loss is attributed to be a result of the early stages of (emim)OAc decomposition. By 300 °C, the system has lost 64.40 % of its total mass leaving only carbonaceous material and poorly-crystalline metal species. The carbonaceous material provided by the dextran is then lost steadily, and is completely consumed at 546 °C. At this point 11.03 % of total mass is present in the system, corresponding to amorphous strontium and niobium species. Further heating reveals a constant mass gain. This gain in mass is a result of the oxidation of niobium (Supplementary information, Figure S1B).

The key feature of the combination of IL and dextran shown here is the exploitation of the super dissociating nature of ILs, allowing the formation of perfect homogenous solutions via the interaction of hard anions of the IL with the metal cations, and the extra chelation provided by a non-specific chelating agent such as dextran. We found that varying the amount of niobium in the reaction enabled us to control the stoichiometry finely and consistently, to produce four distinct stoichiometries of strontium niobate. Previously, it has been shown that it is possible to maintain the same phase composition and yet vary the stoichiometry in (K, Na) (Nb, Ta)O_3 materials[33,34]. Here we explore analogous syntheses in the strontium niobate system. The specific Sr/Nb molar ratios are: 2:1 for $Sr_4Nb_2O_9$, 1.1:1 to 0.9:1 for $Sr_5Nb_4O_{15}$, 0.8:1 to 0.7:1 for $Sr_2Nb_2O_7$, 0.5:1 to 0.3:1 for $SrNb_2O_6$ and 0.11:1 for $SrNb_6O_{16}$. The addition of dextran followed by calcination at 1000 °C for 2 hrs in a 5 °C/min ramp ratio enabled two phases with a stoichiometry X/Y >1 to be obtained, i.e. $Sr_4Nb_2O_9$ and $Sr_5Nb_4O_{15}$ (Figure 2).

The phase $Sr_4Nb_2O_9$ (Fig. 2A) can exhibit different crystalline structures according to the temperature of synthesis. In this work, syntheses were carried out at 1000 °C, therefore, the phase is monoclinic with a symmetry group P21/n. In the case of $Sr_5Nb_4O_{15}$ (Fig. 2B), this possessed a trigonal crystal structure with the symmetry group $P\bar{3}c1$. The remaining phases in this work have the stoichiometry X/Y <1, viz. $Sr_2Nb_2O_7$ (Fig. 2C), $SrNb_2O_6$ (Fig. 2D) and $SrNb_6O_{16}$ (Fig. 2E). The phase (2-2-7) is orthorhombic with the symmetry group Cmc21 and it is determined that (1-2-6) exists as a monoclinic phase with space group P21/c. (1-6-16) has an

View Article Online
DOI: 10.1039/C7CE01298E

orthorhombic array with Pmm2 symmetry group. All diffraction peaks in the patterns can be indexed to pure phases with exception of (1-6-16). In this case, Rietveld refinement shows that the desired phase is present as 95.7% of the sample, whereas 4.3% corresponds to (1-2-6) and niobium oxide (Figure 2). This last crystalline phase was synthesized under a 1:9 Sr/Nb molar ratio, which explains the appearance of the niobium-rich phase (1-2-6) and the impurity on the powder X-ray diffraction pattern, yet this molar ratio almost fully supresses the growth of any other crystal phase. SEM studies show (Figure 3 and Supplementary information, Figure S2) that this type of synthesis results in a polycrystalline aggregate exhibiting the same macromorphology in every single crystal phase. EDXA shows that in each case, strontium and niobium are homogeneously distributed throughout the material (Figure 3). A quantitative compositional analysis of each crystal phase is also presented (Supplementary information, Figure S3). The homogeneity afforded by the IL/Dextran mixture clearly results in a phase-pure material through the facile mass transport of species during the synthesis.

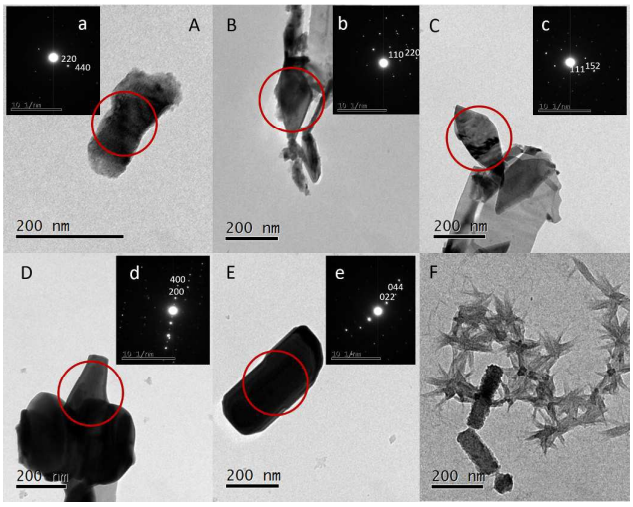

Figure 4. Transmission Electron Microscopy Images and their respective SAED patterns of: A/a) $Sr_4Nb_2O_9$, B/b) $Sr_5Nb_4O_{15}$, C/c) $Sr_2Nb_2O_7$, D/d) $SrNb_2O_6$, E/e) $SrNb_6O_{16}$ and F) Rod and star shape crystals.

In contrast with SEM studies of the macromorphology, TEM images (Figure 4) show some differences in the crystallite morphology, in particular for the phase (4-2-9) (Supplementary information, Figure S4) where a net of nanoparticles-like are commonly seen. From the samples over the ratio 1:2 Sr/Nb most of the final product can be identified as plate-like and rod morphologies, however, star and needle-like morphologies are observed in all syntheses.

In conclusion, the use of an IL/Dextran synthetic method has shown to be a very good technique in the synthesis of high yields of phase-pure metal oxides of desired stoichiometries. The non-specific chelation and subsequent carbonization of the organic species in the calcination step are crucial in achieving this as it restricts inorganic oxide growth to the nanoscale, prevents sintering and provides a reducing atmosphere to enable the fine control of stoichiometry through simply varying the strontium:niobium ratio at the start of the synthesis.

Conflict of interest

There are no conflicts to declare.

Acknowledgements

The authors would like to acknowledge the Engineering and Physical Sciences Research Council (EPSRC), UK (grant EP/G036780/1), and the Bristol Centre for Functional Nanomaterials for project funding. O.G. would like to thank Consejo Nacional de Ciencia y Tecnología (Conacyt), Mexico for the provision of a scholarship.

Notes and references

1 R. E. Cohen, Nature, 1992, 358, 136–138.
2 V. P. Thakare, O. S. Game and S. B. Ogale, J. Mater. Chem. C, 2013, 1, 1545.
3 F. Lichtenberg, A. Herrnberger and K. Wiedenmann, Prog. Solid State Chem., 2008, 36, 253–387.
4 Z. L. Wang, Adv. Mater., 2012, 24, 4632–46.
5 T. Adschiri, Y. Hakuta and K. Arai, Ind. Eng. Chem. Res., 2000, 39, 4901–4907.
6 Q. Sun, Q. Gu, K. Zhu, R. Jin, J. Liu, J. Wang and J. Qiu, Sci. Rep., 2017, 7, 42274.
7 Q. Gu, K. Zhu, N. Zhang, Q. Sun, P. Liu, J. Liu, J. Wang and Z. Li, J. Phys. Chem. C, 2015, 119, 25956–25964.
8 Z. Li, B. Hou, Y. Xu, D. Wu, Y. Sun, W. Hu and F. Deng, J. Solid State Chem., 2005, 178, 1395–1405.
9 H. Wang, L. Wang, J. Liu, B. Wang and H. Yan, Mater. Sci. Eng. B, 2003, 99, 495–498.
10 X. Liu, N. Fechler and M. Antonietti, Chem. Soc. Rev., 2013, 42, 8237–65.
11 C. J. Brinker and G. W. Scherer, Sol-Gel Science: The Physics and Chemistry of Sol-Gel Processing, Elsevier Science, 2013.
12 A. E. Danks, S. R. Hall and Z. Schnepp, Mater. Horiz., 2016, 3, 91–112.
13 M. Armand, F. Endres, D. R. MacFarlane, H. Ohno and B. Scrosati, Nat. Mater., 2009, 8, 621–9.
14 Z. Ma, J. Yu and S. Dai, Adv. Mater., 2010, 22, 261–85.
15 J. Dupont, G. S. Fonseca, A. P. Umpierre, P. F. P. Fichtner and S. R. Teixeira, J. Am. Chem. Soc., 2002, 124, 4228–4229.
16 A. Taubert, Angew. Chemie, 2004, 116, 5494–5496.
17 H. Zhu, J.-F. Huang, Z. Pan and S. Dai, Chem. Mater., 2006, 18, 4473–4477.
18 T. Nakashima and N. Kimizuka, J. Am. Chem. Soc., 2003, 125, 6386–7.
19 Y. Wang, S. Maksimuk, R. Shen and H. Yang, Green Chem., 2007, 9, 1051.

View Article Online
DOI: 10.1039/C7CE01298E

20 Y. Jiang and Y.-J. Zhu, J. Phys. Chem. B, 2005, 109, 4361–4.
21 C. J. Adams, A. E. Bradley and K. R. Seddon, Aust. J. Chem., 2002, 54, 679–681.
22 B. Lee, H. Luo, C. Y. Yuan, J. S. Lin and S. Dai, Chem. Commun., 2004, 0 (2), 240–241.
23 D. C. Green, S. Glatzel, A. M. Collins, A. J. Patil and S. R. Hall, Adv. Mater., 2012, 24, 5767–72.
24 D. Y. Wan, Y. L. Zhao, Y. Cai, T. C. Asmara, Z. Huang, J. Q. Chen, J. Hong, S. M. Yin, C. T. Nelson, M. R. Motapothula, B. X. Yan, D. Xiang, X. Chi, H. Zheng, W. Chen, R. Xu, Ariando, A. Rusydi, A. M. Minor, M. B. H. Breese, M. Sherburne, M. Asta, Q.-H. Xu and T. Venkatesan, Nat. Commun., 2017, 8, 15070.
25 X. Xu, C. Randorn, P. Efstathiou and J. T. S. Irvine, 2012.
26 M. Shida, K. Akiyama, I. Nagano, Y. Murakami and S. Ohta, Key Eng. Mater., 2006, 317–318, 517–520.
27 S. Kamba, J. Petzelt, E. Buixaderas, D. Haubrich, P. Vaněk, P. Kužel, I. N. Jawahar, M. T. Sebastian and P. Mohanan, J. Appl. Phys., 2001, 89, 3900.
28 J. K. Yamamoto and A. S. Bhalla, Mater. Lett., 1991, 10, 497–500.
29 N. Ishizawa, F. Marumo, T. Kawamura and M. Kimura, Acta Crystallogr. Sect. B Struct. Crystallogr. Cryst. Chem., 1975, 31, 1912–1915.
30 Y. Zhou, Q. Ma, M. Lü, Z. Qiu, A. Zhang and Z. Yang, Mater. Sci. Eng. B, 2008, 150, 66–69.
31 Y. Fujimori, N. Izumi, T. Nakamura and A. Kamisawa, Jpn. J. Appl. Phys., 1998, 37, 5207–5210.
32 O. G. D'yachenko, S. Y. Istomin, A. M. Abakumov and E. V. Antipov, Inorg. Mater., 2000, 36, 247–259.
33 L. Bai, K. Zhu, L. Su, J. Qiu and H. Ji, Mater. Lett., 2010, 64, 77–79.
34 H. Gu, K. Zhu, X. Pang, B. Shao, J. Qiu and H. Ji, Ceram. Int., 2012, 38, 1807–1813.
35 D. Walsh, L. Arcelli, T. Ikoma, J. Tanaka and S. Mann, Nat. Mater., 2003, 2, 386–390.
36 D. Walsh, S. C. Wimbush and S. R. Hall, Supercond. Sci. Technol., 2009, 22, 15026.